

# Green Chemistry

Accepted Manuscript



This is an *Accepted Manuscript*, which has been through the Royal Society of Chemistry peer review process and has been accepted for publication.

*Accepted Manuscripts* are published online shortly after acceptance, before technical editing, formatting and proof reading. Using this free service, authors can make their results available to the community, in citable form, before we publish the edited article. We will replace this *Accepted Manuscript* with the edited and formatted *Advance Article* as soon as it is available.

You can find more information about *Accepted Manuscripts* in the [Information for Authors](#).

Please note that technical editing may introduce minor changes to the text and/or graphics, which may alter content. The journal's standard [Terms & Conditions](#) and the [Ethical guidelines](#) still apply. In no event shall the Royal Society of Chemistry be held responsible for any errors or omissions in this *Accepted Manuscript* or any consequences arising from the use of any information it contains.



[www.rsc.org/greenchem](http://www.rsc.org/greenchem)

# Integrated Process for the Catalytic Conversion of Biomass-Derived Syngas into Transportation Fuels

Vanessa Lebarbier Dagle, Colin Smith, Matthew Flake, Karl O. Albrecht, Michel J. Gray  
Karthikeyan K. Ramasamy, and Robert A. Dagle\*

*Energy and Environmental Directorate, Institute for Integrated Catalysis, Pacific Northwest  
National Laboratory, Richland, WA 99352, USA*

Submitted to *Green Chemistry*

*September 2015*

\*Corresponding author: [Robert.Dagle@pnl.gov](mailto:Robert.Dagle@pnl.gov)

## Abstract

Efficient synthesis of renewable fuels that will enable cost competitiveness with petroleum-derived fuels remains a grand challenge. In this paper, we report on an integrated catalytic approach for producing transportation fuels from biomass-derived syngas. This novel process represents an alternative to conventional fuel synthesis routes (e.g., Fischer-Tropsch, Methanol-to-Gasoline) that have drawbacks, particularly at the scale of biomass. Composition of the resulting hydrocarbon fuel can be modulated to produce predominantly middle distillates, which is constantly increasing in demand compared to gasoline fraction. In this process biomass-derived syngas is first converted over an Rh-based catalyst into a complex aqueous mixture of condensable  $C_2^+$  oxygenated compounds (predominantly ethanol, acetic acid, acetaldehyde, ethyl acetate). This multi-component aqueous mixture then is fed to a second reactor loaded with a  $Zn_xZr_yO_z$  mixed oxide catalyst, which has tailored acid-base sites, to produce an olefin mixture rich in isobutene. The olefins then are oligomerized using a solid acid catalyst (e.g., Amberlyst-36) to form condensable olefins with molecular weights that can be targeted for gasoline, jet, and/or diesel fuel applications. The product rich in long-chain olefins ( $C_7^+$ ) is finally sent to a fourth reactor required for hydrogenation of the olefins into paraffin fuels. Simulated distillation of the hydrotreated oligomerized liquid product indicates that ~75% of the hydrocarbons (isoparaffins and cyclic compounds) are in the jet-fuel range. Process optimization for the oligomerization step could further improve yield to the jet-fuel range. All of these catalytic steps have been demonstrated in sequence, thus providing proof-of-concept for a new integrated process for the production of drop-in biofuels. Overall, we demonstrate approximately 41% carbon efficiency for converting syngas into jet-range hydrocarbons. This unique and flexible process does not require external hydrogen and also could be applied to non-syngas derived

feedstock, such as fermentation products (e.g., ethanol, acetic acid, etc.), other oxygenates, and mixtures thereof containing alcohols, acids, aldehydes and/or esters.

**Keywords:** biomass, syngas, biofuel, catalyst, mixed oxides, oligomerization, mixed oxygenates, ethanol, isobutene, jet fuel

## Introduction

Although still the main resource for transportation fuels, fossil fuels are becoming less attractive as a carbon source because they are being depleted and contribute to climate change. A more environmentally friendly and secure long-term solution would consist of an array of vehicle energy sources ranging from electricity, hydrogen, solar energy, and biofuels. Biomass-derived hydrocarbon fuels are attractive because they are CO<sub>2</sub> neutral and provide a renewable carbon resource. Biomass conversion to fuels can be achieved either through thermochemical routes (e.g., pyrolysis, gasification) or biochemical routes (e.g., fermentation).<sup>1,2</sup> Thermochemical processing has several advantages relative to biochemical processing, including greater feedstock flexibility, conversion of both carbohydrate and lignin into products, faster reaction rates, and the ability to produce a diverse selection of fuels.<sup>3</sup> Among the thermochemical routes, one can distinguish between gasification and direct liquefaction routes, such as fast pyrolysis, hydrothermal liquefaction, or hydrolysis that produce a bio-oil directly.<sup>1,2</sup> Fast pyrolysis of biomass into bio-oils and subsequent catalytic hydroprocessing are considered to be among the most viable technologies available to produce liquid biofuels through thermochemical means.<sup>4</sup> Indeed, improved thermal efficiencies are achieved relative to liquid fuels production from gasification followed by Fischer-Tropsch Synthesis or ethanol synthesis.<sup>1</sup> However, one major drawback to this approach is the limited possible use of the finished fuel because of its composition. Hydro-processed bio-oils typically contain large amounts of cyclic components and up to 35% aromatics and 40 to 55% cycloparaffins.<sup>5</sup> In addition, the upgrading step via hydro-processing requires large quantities of externally provided hydrogen.

Biomass gasification is a process by which biomass reacts with air, O<sub>2</sub>, and/or steam at high temperatures (e.g., 900 to 1100°C) to produce a syngas product comprising primarily H<sub>2</sub>, CO, CO<sub>2</sub>, and N<sub>2</sub>. The syngas can subsequently be cleaned of impurities (e.g., sulfur, tar) and then

used to produce fuels and/or chemicals via a variety of possible routes,<sup>1</sup> with the most common processes being Fischer-Tropsch Synthesis, Methanol-to-Gasoline, and Mobil Olefins-to-Gasoline-and-Distillate.<sup>1</sup> Because of the high costs and complexity associated with these processes, the production cost of finished fuel cannot currently compete with petroleum-derived fuel. Yield and selectivity towards more desirable diesel- and jet-range hydrocarbons should also be maximized in biomass conversion processes as the demand for middle distillates (e.g., jet and diesel fuels) in comparison to gasoline fractions is increasing.<sup>6</sup>

Recently, companies such as GEVO,<sup>7</sup> Honeywell's UOP<sup>8</sup>, and Cobalt<sup>9</sup> have been investigating the possibility of producing jet-fuel range hydrocarbons fuel from biomass sources via (iso- or n-) butanol as an intermediate. Butanol (iso- or n-) can be easily dehydrated into butene (iso- or n-) that can be further oligomerized into dimers (C<sub>8</sub>), trimers (C<sub>12</sub>), and tetramers (C<sub>16</sub>), and then hydrogenated into jet-fuel range hydrocarbons. Dumesic et al.<sup>10</sup> have also proposed an integrated process for producing transportation fuels including jet fuel via catalytic conversion of  $\gamma$ -valerolactone (GVL). In this process, GVL produced from biomass-derived carbohydrates is converted into butene that can be oligomerized into long-chain olefins (C<sub>8</sub><sup>+</sup>) and then hydrogenated into long-chain paraffins. All these processes for biojet fuel synthesis involve the use of a single alcohol feedstock or olefin intermediate.

In recent years, much research has been performed in developing catalysts for the production of ethanol from biomass-derived syngas.<sup>11,12,13,14</sup> Supported Rh-based catalysts have the highest activity and selectivity for the formation of ethanol and other C<sub>2</sub><sup>+</sup> oxygenates from syngas because of their ability to catalyze both CO dissociation and CO insertion.<sup>15</sup> However, the Rh-based catalysts typically produce oxygenates other than just alcohols within their product slate. C<sub>2</sub><sup>+</sup> oxygenates produced include predominately acetic acid, acetaldehyde, and ethyl acetate in

addition to ethanol.<sup>15-18</sup> Finding utility for this mixed oxygenates stream and without the need for costly separations is problematic.<sup>19</sup> Here, we report on a unique upgrading of this aqueous oxygenated mixture to produce middle distillates utilizing a  $Zn_xZr_yO_z$  mixed-oxide catalyst. This catalyst was previously reported useful for the conversion of ethanol<sup>20, 21</sup> and more recently by our group for the conversion of a multitude of  $C_2^+$  oxygenates (e.g., ethanol, acetic acid, acetaldehyde, ethyl acetate) to isobutene-rich olefins.<sup>22</sup>

In this report, we propose a new process, using a complex mixture of oxygenated compounds as intermediates, to produce jet-fuel range hydrocarbons from biomass-derived syngas. Two different processing schemes have been examined, and block flow diagrams for both schemes are shown in Figure 1. For both cases, biomass-derived syngas is first converted into a mixture of alcohols and other oxygenates over a Rh-based catalyst (Reactor R1) developed at Pacific Northwest National Laboratory (PNNL).<sup>16</sup> Then, the complex mixture of oxygenated compounds is fed to Reactor R2, which is installed in series and loaded with a  $Zn_xZr_yO_z$  catalyst, thus producing an olefin mixture and other light products (primarily  $H_2$  and  $CO_2$ ). For “case A,” both the olefin mixture and the gaseous product are fed to Reactor R3, which is loaded with an Amberlyst-36 solid acid catalyst. This scheme represents the case with minimal separations. For “case B,” light products are separated using a lean oil scrubber and the olefin mixture is processed in Reactor R3. The resulting long-chain olefin product is finally hydrogenated into paraffin fuel in Reactor R4 using a 3% Pt/ $Al_2O_3$  hydrogenation catalyst. In this process, the  $H_2$  product is used so externally supplied  $H_2$  is not needed. In this report, we also disclose catalytic performance results for the  $Zn_xZr_yO_z$  mixed-oxide catalyst used for the conversion of  $C_2^+$  mixed oxygenates, derived from an Rh-based syngas conversion catalyst, to isobutene-rich mixed olefins. Then, we demonstrate oligomerization of this mixed olefin to a jet-fuel range

hydrocarbon. Furthermore, we comparatively assess catalytic performance results for solid-acid catalysts (HZSM-5, HY, and Amberlyst-36) for oligomerization under industrially relevant conditions.

## Experimental

### Catalyst preparation

An Rh-based catalyst (catalyst H-A) was prepared by incipient wetness impregnation for converting syngas to mixed oxygenates. Details regarding the synthesis can be found in a previous report published by PNNL.<sup>16</sup> For conversion of mixed oxygenates to olefins, the  $Zn_1Zr_{10}O_2$  mixed-oxide catalyst was synthesized via incipient wetness impregnation of  $Zr(OH)_4$  with an aqueous solution of  $Zn(NO_3)_2 \cdot 6H_2O$ .<sup>23,24</sup> Prior to impregnation, the  $Zr(OH)_4$  support was dried overnight at 105°C. After impregnation, the catalyst was dried overnight at room temperature followed by 4 hours at 105°C, calcining at 400°C for 2 hours, and final calcining at 550°C for 3 hours. The molar ratio of Zn:Zr was equal to 1:10. For the oligomerization of olefins, three commercial catalysts were tested: 1) an Amberlyst-36 resin (Romm and Haas), 2) a HZSM-5 zeolite (Zeolyst international,  $SiO_2:Al_2O_3 = 30$ , CBV 3024E), and 3) an HY zeolite (Zeolyst international,  $SiO_2:Al_2O_3 = 30$ , CBV 720). The two zeolites were calcined under air at 500°C for 4 hours prior to use.

### Reactivity Measurements

#### Mixed oxygenates conversion to an isobutene-rich olefin mixture (Reactor R2)

Catalytic activity tests for the conversion of aqueous oxygenated feeds were conducted in a 4.57-mm inner-diameter (ID) fixed-bed reactor loaded with 1.0 g of  $Zn_1Zr_{10}O_2$  mixed-oxide catalyst. A K-type thermocouple was placed in the middle of the reactor bed for measurement of



the catalyst bed temperature. Temperature gradients were minimized through the use of an electrical resistance heating block. Prior to testing, catalysts were activated in situ at 450°C for 8 hours under N<sub>2</sub> introduced into the system using Brooks mass flow controllers (5850E series). Then, the aqueous oxygenated mixture was fed into the system using an ISCO syringe pump and a vaporizer consisting of 6.6-mm ID stainless steel tubing filled with quartz beads. The effects of conversion and selectivity were measured over a range of temperatures (375 to 450°C), pressures (1 to 21 bar), and gas-hour-space-velocities (GHSV = 340 to 7500 h<sup>-1</sup>) as specified in the text. Gaseous effluents were analyzed online using an Inficon micro-gas chromatograph (GC) (Model 3000A) equipped with MS-5A, Plot U, alumina, and OV-1 columns and a thermal conductivity detector. Liquid products were analyzed offline using liquid chromatography. When catalyst regeneration was performed, the catalysts were treated in situ under flowing 5% O<sub>2</sub>/He at 550°C for 8 hours. Upon completion, the catalyst was cooled to the desired reactor operating temperature under N<sub>2</sub>.

### **Olefin oligomerization (Reactor R3)**

The reactivity measurements for the oligomerization of olefins were conducted in the gas phase using a 9.1-mm ID fixed-bed reactor. A K-type thermocouple placed in the middle of the catalyst bed (60 to 100 mesh catalyst particles) was loaded between two layers of quartz wool. Before each test, the catalysts were pre-treated in situ under N<sub>2</sub> (50 sccm) overnight at 120°C for the Amberlyst-36 or 350°C for the zeolites. Then, the temperature was increased to the desired reaction temperature (140 to 250°C), the N<sub>2</sub> flowrate was adjusted to required flowrate, and the olefin(s) was fed into the system using an ISCO syringe pump and a vaporizer consisting of 6.6-mm ID stainless steel tubing filled with quartz beads. Olefin conversions were measured over a range of WHSVs = 0.5 to 20 hr<sup>-1</sup> at pressures between 5 to 17 bar and temperature equal

to 140°C for the Amberlyst-36 wet and 250°C for the zeolites. Gaseous effluent was analyzed using an Inficon micro GC (Model 3000A) equipped with MS-5A, Plot U, OV-1 columns, and a thermal conductivity detector. Liquid products were analyzed offline using an Agilent GC-mass spectrometer equipped with a DB-5 column. The WHSV was calculated as follows:

$$\text{WHSV} = \text{grams olefin(s) fed per hour} \div \text{grams of catalyst}$$

### **Hydrogenation of olefins (Reactor R4)**

The olefins product from reactor R3 was hydrogenated in an autoclave (reactor R4) loaded with a 3% Pt/Al<sub>2</sub>O<sub>3</sub> (Engelhard) operating at 200°C (ramp 3.3°C/min) with an H<sub>2</sub> pressure of 52 bar for a period of 7.5 hours. Note that an autoclave reactor was used for practical reasons, but a fixed-bed reactor would be used in a commercial application. Simulated distillation of the organic products also was conducted following ASTM D2887.

## **Results and discussion**

### **Syngas conversion to mixed oxygenates (Reactor R1)**

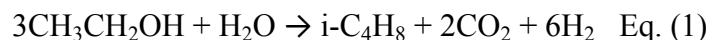
Conversion of biomass-derived syngas to higher alcohols such as ethanol has been the subject of much research.<sup>1, 15</sup> Supported Rh-based catalysts have the highest activity and selectivity for the formation of ethanol and other C<sub>2</sub><sup>+</sup> oxygenates because of their ability to catalyze both CO dissociation and CO insertion.<sup>15</sup> Advances made at PNNL in developing an Rh-based catalyst (Reactor R1, Figure 1) with the goal of achieving high selectivity to C<sub>2</sub><sup>+</sup> oxygenates from syngas have been reported previously.<sup>16-18, 25</sup> This effort culminated in the design of an RhMnIr-based catalyst supported on carbon.<sup>16</sup> This catalyst provides a selectivity to C<sub>2</sub><sup>+</sup> oxygenates of 73% when operating under syngas with a H<sub>2</sub>:CO molar ratio of 1.3 (containing

3 mol% CO<sub>2</sub>), at 80 atm, 260°C, and a GHSV of 13,000 L/kg<sub>cat</sub>/hr (see Table 1 for testing condition details). As disclosed in our earlier report, this catalyst was evaluated for stability and tested continuously for 2300-plus hours.<sup>16</sup> Condensed liquid product was periodically collected for analysis during the course of this duration testing. At the completion of the 2300-plus hour evaluation, all of the liquid samples were combined, analyzed, and the resulting complex mixture composition is shown in Table 2. This oxygenated mixture was used as feed for Reactor R2 (Figure 1), which produces the isobutene-rich olefin stream.

### **Mixed oxygenates conversion to an isobutene-rich olefin mixture (Reactor R2)**

Conversion of ethanol to isobutene in a single catalytic step, with a high theoretical yield of 83%, was recently reported by Sun<sup>20, 26</sup> and Liu<sup>21</sup> when using a Zn<sub>x</sub>Zr<sub>y</sub>O<sub>z</sub> mixed-oxide type catalyst with balanced acid-base sites. Traditionally, catalysts designed for acetone production from ethanol<sup>27, 28</sup> or isobutene production from acetone<sup>29-31</sup> are separately employed. Only recently were these reactions demonstrated in tandem when using Zn<sub>x</sub>Zr<sub>y</sub>O<sub>z</sub> that selectively facilitates the ethanol-to-isobutene cascade reaction. A simplified reaction mechanism is shown in Figure 2.<sup>22</sup> Ethanol first undergoes ethanol dehydrogenation and ketonization reactions thus producing acetone. ZnO addition offers the necessary basic sites while also suppressing most of the strong acid sites responsible for undesirable ethanol dehydration.<sup>20, 26</sup> Acetone then undergoes aldol condensation and C-C cleavage over acid sites, while the formation of acetone decomposition products (CH<sub>4</sub> and CO<sub>2</sub>) is largely suppressed.<sup>20, 26</sup> It was shown that acetone acts as the key intermediate in ethanol-to-isobutene, and the reaction is limited by the acetone-to-isobutene conversion.<sup>26</sup> It should be noted that metisyl oxide is a commonly considered intermediate in the acetone-to-isobutene reaction (as illustrated in Figure 2).<sup>22, 26</sup> However, recent isotopic labelling experiments performed by Sun et al. when using a Zn<sub>x</sub>Zr<sub>y</sub>O<sub>z</sub> catalyst

characterized by Lewis acid-base pairs (and devoid of Brønsted acidity) indicate diacetone alcohol directly decomposes to a surface acetate, whereby the dehydration intermediate metisyl oxide was largely not formed.<sup>26</sup> In either case isobutene is ultimately produced. The idealized net reaction for the ethanol-to-isobutene reaction is shown in Equation 1. Byproducts include H<sub>2</sub> and CO<sub>2</sub> and the theoretical carbon selectivity is 66.7 mol%.



In our earlier study, we reported on the extended utility of a Zn<sub>x</sub>Zr<sub>y</sub>O<sub>z</sub> catalyst for conversion of additional oxygenates that, in addition to ethanol, include acetic acid, acetaldehyde, ethyl acetate, and mixtures thereof.<sup>22</sup> Ethanol, acetic acid, and acetaldehyde all result in similar product distributions, which is not unexpected as acetic acid and acetaldehyde are intermediates within the reaction network from ethanol as illustrated in Figure 2. Ethyl acetate in the presence of water undergoes hydrolysis to form ethanol and acetic acid, both of which then proceed along the same reaction pathway thus rendering a similar product distribution with isobutene and CO<sub>2</sub> being the primary products.<sup>22</sup> In addition, we also demonstrated scalability to higher carbon number analogs. For example, propanol was found to produce branched C<sub>6</sub> olefins over Zn<sub>x</sub>Zr<sub>y</sub>O<sub>z</sub> in a pathway analogous as that followed for the conversion of ethanol to isobutene. Formation of 2-butanone was demonstrated to be the rate limiting ketone intermediate analogous to acetone in the case of ethanol. Thus, in our prior report, we establish the versatility and efficiency of the Zn<sub>x</sub>Zr<sub>y</sub>O<sub>z</sub> catalyst for converting complex aqueous mixtures of oxygenated compounds into olefins, and we discuss in detail the reaction mechanism.<sup>22</sup> In this paper, we demonstrate the use of an actual aqueous mixed oxygenated product derived from the RhMnIr-based syngas conversion catalyst as feedstock. We also explore the effects of industrially relevant conditions such as temperature, GHSV, and pressure on catalytic performance.

Reactor R2 (Figure 1) was loaded with  $Zn_1Zr_{10}O_2$  catalyst and the effects of temperature, pressure, and GHSV were evaluated. Figure 3 presents the effect of temperature on product selectivity at almost full conversion ( $\geq 94\%$ ). Conversion of the complex oxygenate feed mixture (Table 2) over  $Zn_1Zr_{10}O_2$  leads primarily to the formation of olefins (predominantly butenes with some ethene, propene, and pentenes), ketones (mainly acetone, with some 2-butanone), and  $CO_2$ . As the temperature increases from 375 to 450°C, selectivity for ketones decreases significantly while selectivity for olefins increases. This finding supports the proposed mechanism in which the  $C_2$  oxygenates (e.g., ethanol, acetic acid, acetaldehyde) are rapidly converted into ketones (e.g., acetone) and a second, rate-limiting step in which ketones are transformed into olefins.<sup>22</sup> Ethyl acetate is believed to hydrolyze to ethanol and acetic acid, thereby converting along the same pathway.<sup>22</sup> The  $CO_2$  selectivity is stable at approximately 35% over the range of temperatures investigated. Production of  $CO_2$  results from conversion of ethanol, acetaldehyde, and acetic acid, and it is required as dictated by stoichiometry. Carbon dioxide also is produced from methanol as a result of methanol steam reforming.<sup>22</sup> While the methane selectivity is low at approximately 2% at 425°C, it increases to approximately 3.5% at 450°C, and substantially further at elevated temperatures. Decomposition of acetone at higher temperatures is speculated to be the source of methane production.<sup>22</sup> At 450°C, a 48% yield to olefins was attained, which corresponds to approximately 70% of the stoichiometric yield. Further parameters were investigated while operating Reactor R2 at 450°C.

Product selectivity as a function of GHSV while operating at 450°C and at 100% carbon conversion are shown in Figure 4. When the GHSV decreases from 7400 to 1900  $h^{-1}$ , butene selectivity increases from ~25 to 33%, and acetone selectivity decreases from ~23 to 6%.

Decreasing GHSVs favor conversion of ketones into olefins. Methane selectivity also is enhanced at lower GHSV values.

The effect of operating pressure on product selectivity is illustrated in Figure 5. At a GHSV of  $340 \text{ h}^{-1}$ , complete conversion of the acetone intermediate is achieved. Increasing the pressure from 1 to 21 bar has a negative effect on the product distribution as indicated by the butene selectivity, which decreases from ~43 to 32% as propene formation increases from ~12 to 20%. Propene formation is believed to occur as a result of acetone hydrogenation that is facilitated by higher pressures.<sup>22</sup> In our prior study it was demonstrated that for acetic acid conversion over  $\text{Zn}_1\text{Zr}_{10}\text{O}_z$  increasing the amount of  $\text{H}_2$  in the carrier gas corresponded to increasing propene formation.<sup>22</sup> In fact, in the absence of  $\text{H}_2$  no propene was formed.<sup>22</sup> From a practical standpoint, propene is less desired because its oligomerization to  $\text{C}_{13}^+$  is more difficult compared to that of butene. Undesirable methane and CO formation also increases with increasing pressure, but selectivity to each is still relatively low at  $\leq 3\%$  even at 21 bar. The results shown in Figure 5 indicate that lower pressures are preferred to convert the mixed oxygenates into  $\text{C}_4$ -rich olefins. However, in an integrated process, Reactor R2 would likely be operated under some pressure to allow for easier separation of the olefin products from the aqueous phase.

A 24-hour stability test was conducted using the  $\text{Zn}_1\text{Zr}_{10}\text{O}_z$  catalyst at  $450^\circ\text{C}$ , 1 bar, and  $\text{GHSV} = 3700 \text{ h}^{-1}$ . As shown in Figure 6, acetone intermediate product conversion to butenes decreases slightly with time on stream, which is indicative of a catalyst deactivation. However, we have previously shown that the catalyst can be easily regenerated with a mild oxidative treatment under air at  $500^\circ\text{C}$ .<sup>22</sup>

Hence, to optimize the formation of desired olefins product, Reactor R2 should be operated at a temperature (e.g., 450°C) and a GHSV (e.g., 340 h<sup>-1</sup>) that favor conversion of the ketone intermediates. This reaction can be accomplished at atmospheric pressure; however, the system is typically pressurized to some extent to facilitate organic-aqueous separations.

### **Olefin oligomerization (Reactor R3)**

While the oligomerization of olefins is practiced widely in the petrochemical industry, little has been reported regarding the use of mixtures of light olefins to produce a middle distillate. This lack of information thus necessitates studies such as this one to identify suitable catalysts and industrially relevant process conditions.

#### *Oligomerization of isobutene*

The olefin product stream from the mixed oxygenates Reactor R2 contains isobutene as the major olefin product. Thus, isobutene was chosen as a representative feed for oligomerization catalyst screening and parametric investigations. Sulfonic acid resins and zeolites are commonly used catalysts for olefin oligomerization.<sup>32,33,34,35</sup> Catalytic activities of HY zeolite (SiO<sub>2</sub>/Al<sub>2</sub>O<sub>3</sub> = 30), HZSM-5 zeolite (SiO<sub>2</sub>/Al<sub>2</sub>O<sub>3</sub> = 30), and a sulfonic acid resin Amberlyst-36 were evaluated for the oligomerization of isobutene. The catalysts were tested under similar reaction conditions except for the reaction temperature since Amberlyst-36 deteriorates at temperatures above 150°C and higher reaction temperatures are typically required for gas phase oligomerization over zeolites.<sup>10, 36</sup> Product selectivities and C<sub>7</sub><sup>+</sup> yields are presented in Table 3. For both zeolites, undesired C<sub>1</sub>–C<sub>6</sub> compounds were produced, and no C<sub>16</sub><sup>+</sup> compounds were formed. Jet fuel typically contains C<sub>8</sub> up to C<sub>16</sub> hydrocarbons.<sup>37,38</sup> Selectivity toward C<sub>7</sub>–C<sub>12</sub> olefins and paraffins is approximately 74% for both zeolites. As shown in Table 3, olefins are major components

produced over HY, whereas paraffins are the predominant components produced over HZSM-5. Hydrogen transfer is speculated to occur more easily over HZSM-5, leading to hydrogenation of the olefins. Note that no aromatics were detected in the liquid product stream to prove that hydrogen transfer is responsible for the olefins hydrogenation into paraffins. However, during reaction  $H_2$  was detected on-line in the gas stream when the HZSM-5 was used which suggests that hydrogen transfer occurs. Yield toward  $C_7$ – $C_{12}$  hydrocarbons is relatively high and range from 74 to 80% with the zeolites, thus forming hydrocarbons that primarily fall into the gasoline range. Amberlyst-36 distinguishes itself from the zeolites in that a significant amount of branched  $C_{16}^+$  hydrocarbons (i.e., 14.6%) and  $C_8$ – $C_{12}$  cyclic compounds (i.e., 34%) were produced, but no  $C_1$ – $C_6$  hydrocarbons were formed. Note that this is likely due to the fact that the Amberlyst-36 was tested at lower temperature as compared to the zeolites and cracking reactions are less favored. In addition, the  $C_7$ – $C_{12}$  olefins and paraffins are highly branched compared to those products when zeolites were used. This is attributed to the difference in porosity since the branching degree of oligomerization products increases with the pore size<sup>36</sup> and the pores diameter of the Amberlyst 36-wet is equal to 24 nm and is one order of magnitude higher than the one for the zeolites. Because branched long-chain hydrocarbons and cycloalkanes are desirable for jet fuel<sup>38,39</sup> and the yield toward these desired compounds is >98%, Amberlyst-36 is a promising oligomerization catalyst for bio-jet fuel production; therefore, it was chosen as the oligomerization catalyst for Reactor R3 of the integrated process. The effect of the process conditions such as WHSV and pressure were investigated.

The effect of the WHSV on selectivity was investigated at full conversion, 17 bar, and 140°C (Figure 7). The  $C_7$ – $C_{12}$  olefin selectivity increases from 45 to 60% when the WHSV increases from 0.6 to 2.6  $h^{-1}$ . On the contrary, the  $C_{16}$  olefin selectivity and the  $C_8$ – $C_{12}$  cyclic compound



selectivity decreased with an increase of WHSV. Note that cracking is negligible over the range of WHSVs studied because selectivity toward  $C_1$ – $C_6$  paraffin is  $\leq 2\%$ . These results show that the nature of the hydrocarbon fuel (gasoline or jet fuel) can be modulated by varying space velocity. While higher GHSVs favor the formation of a gasoline-range fuel, lower GHSVs can be used to produce longer hydrocarbon chains (i.e.,  $C_{16}$  olefins) and cyclic compounds appropriate for jet fuel.<sup>40</sup> Figure 8 presents the evolution of selectivity with increasing pressure from 7 to 17 bar over Amberlyst-36 at full conversion, 140°C, and  $WHSV = 1.3 \text{ h}^{-1}$ . The selectivity toward  $C_1$ – $C_6$  paraffins is negligible ( $< 2\%$ ), and the selectivity toward other product types (i.e.,  $C_7$ – $C_{12}$  olefins,  $C_8$ – $C_{12}$  cyclic compounds and  $C_{16}$  olefins) is very similar for pressures between 7 and 17 bar. It is probable that under the conditions tested the  $C_7$ – $C_{12}$  products are in condensed phase. A pressure equal to 7 bar seems sufficient to produce long-chain hydrocarbons ( $C_7^+$ ) when using isobutene as a feed. For practical applications, it is essential to maintain high selectivity toward desired long-chain olefins ( $C_7^+$ ) over time with minimal deactivation. The evolution of selectivity at 100% conversion and for a period of 70 hours was demonstrated, and results are shown in Figure 9 with the reactor operating at 140°C, 17 bar,  $WHSV = 1.3 \text{ h}^{-1}$ , and 100% conversion. The catalyst selectivity is very stable with time-on-stream (TOS) over this 70-hour duration.

Amberlyst-36 was found to be the preferred oligomerization catalyst over HZSM-5 and HY zeolites. Operating parameters were investigated using isobutene as feed, and conditions favorable to the formation of jet-range hydrocarbons ( $T = 140^\circ\text{C}$ ,  $P = 17 \text{ bar}$ ,  $WHSV = 0.6 \text{ h}^{-1}$ ) were established. This catalyst system was studied further for oligomerization using the isobutene-rich olefin mixtures derived from the mixed oxides catalyst (Reactor R2).

#### *Oligomerization of olefin mixtures*

For the integrated process described here, two cases were considered for the oligomerization step. For “case A,” the olefin products derived from Reactor R2 remain in the gas phase while water is condensed out. This gas phase, which contains the olefins, H<sub>2</sub>, CO<sub>2</sub>, and traces of both CO and C<sub>1</sub>–C<sub>3</sub> alkanes, is sent directly to the oligomerization step (Reactor R3). This scheme represents the case with minimal separations. For “case B,” the olefin products from Reactor R2 are separated using a lean oil scrubber and thus separated from the water and gaseous effluent (H<sub>2</sub> + CO<sub>2</sub> + CO + C<sub>1</sub>–C<sub>3</sub> alkanes). In this scenario, only the scrubbed olefin product is fed to the oligomerization Reactor R3. Process conditions for the oligomerization step (Reactor R3) were evaluated for both cases.

First, “case A” is considered where the product mixture from Reactor R2 after water separation is directly sent to the oligomerization reactor (Reactor R3), which is loaded with Amberlyst-36 and operated at 140°C. Olefin conversion versus TOS, when operating at 7 bar and WHSV = 0.05–0.1 h<sup>-1</sup>, is shown in Figure 10. Olefin conversion rapidly decreases with TOS. For example, conversion decreases from 93% (TOS = 4 hours) to 80% (TOS = 22 hours) when operating at WHSV = 0.1 h<sup>-1</sup>. Interestingly, when the pressure is increased to 14 bar, the olefin conversion is significantly more stable and decreases only slightly from 95% (TOS = 48 hours) to 93% (TOS = 70 hours). It is speculated that at lower pressure (i.e. 7 bar) the C<sub>7</sub>–C<sub>12</sub> products are present in gas phase and they polymerize into higher molecular weight hydrocarbons blocking the active sites. On the contrary at higher pressure (i.e. 14 bar) the C<sub>7</sub>–C<sub>12</sub> hydrocarbons are present in condensed phase and they do not polymerize. A further investigation would be required to validate this hypothesis. One also can see from Table 4 that selectivity toward the C<sub>7</sub>–C<sub>12</sub> olefins + paraffins product (67.6%) is the highest at 14 bar, implying that oligomerization is favored at higher pressure. Note that this result is in agreement with findings reported

previously for n-butene oligomerization over Ni-HZSM-5 where the trimerization was favored at 40 bar as compared to 10 to 20 bar.<sup>41</sup> In “case A” reported here, C<sub>12</sub><sup>+</sup> olefin products were not observed, thus the hydrocarbon product slate falls into the gasoline range. The olefin mixture was highly diluted in the H<sub>2</sub> + CO<sub>2</sub> gas mixture, and the partial pressure of the olefins is believed to be too low to favor the oligomerization. It is worth mentioning that the H<sub>2</sub> and CO<sub>2</sub> both present in high concentrations in the gas stream are not believed to affect the catalyst stability or selectivity because separate experiments presented Table 7 and conducted in the presence of isobutene + H<sub>2</sub> or CO<sub>2</sub> as a feed mixture showed similar results as to when the feed stream contains only isobutene. The addition of H<sub>2</sub> and CO<sub>2</sub> in the feed does, however, add considerable diluent thus requiring larger oligomerization reactor size than if they were omitted.

Next, “case B” is considered where H<sub>2</sub> and CO<sub>2</sub> are separated from the product stream prior to oligomerization. In this case, only olefins produced from Reactor R2 are sent to the oligomerization Reactor R3 after being scrubbed out. The olefin product stream from Reactor R2 primarily contains butenes, but pentenes and an appreciable amount of propene formed in part due to the higher operating pressure used for Reactor R2 also are present. Because the butene\propene\pentene ratio changes depending on how reactor R2 is operated, three different olefin mixtures were evaluated, and the results are shown in Table 5. Low WHSV (<1 h<sup>-1</sup>) was used to favor the formation of longer-chain (C<sub>12</sub><sup>+</sup>) olefins. The results presented in Table 6 for each feed mixture show the presence of a large amount of C<sub>7</sub>–C<sub>12</sub> olefins + paraffins (≥49%) and C<sub>8</sub>–C<sub>12</sub> cyclic compounds (≥19%), as well as some C<sub>1</sub>–C<sub>6</sub> olefins product (3-13%) and some C<sub>12</sub><sup>+</sup> olefins (4-15% and mainly C<sub>13</sub>–C<sub>16</sub>). An increase of the C<sub>1</sub>–C<sub>6</sub> olefins products and C<sub>12</sub><sup>+</sup> olefins is observed with a decrease of the WHSV. Correspondingly, the C<sub>7</sub>–C<sub>12</sub> olefins production increases with increasing WHSV. The C<sub>8</sub>–C<sub>12</sub> cyclic hydrocarbon selectivity is

relatively stable within the range of WHSVs studied between ~25 and 30%. This is in agreement with our result obtained for the oligomerization of isobutene (Figure 7) and confirms that lower WHSVs ( $<1 \text{ h}^{-1}$ ) favor the formation of  $\text{C}_{12}$ – $\text{C}_{16}$  hydrocarbons that are desired for jet fuel. It is also shown that the composition of the feed mixture affects the product selectivity.

Comparing results between the use of Mixtures A and B as feedstocks reveals the consequences that the mixed oxide derived olefin product composition (Reactor R3) has on subsequent oligomerization performance (Reactor R4). At comparable WHSVs, more propene and less pentene in the feed leads to a decrease of both the  $\text{C}_{12}^+$  olefins and  $\text{C}_1$ – $\text{C}_6$  olefin product selectivities. Thus, both the feed composition and WHSV value can significantly impact hydrocarbon distribution of the oligomerization step. The olefin product obtained after oligomerization of Mixture B was hydrogenated in Reactor R4, which was loaded with 3%Pt/ $\text{Al}_2\text{O}_3$  and operated at 200°C and  $P = 52$  bar for a period of 7.5 hours. Simulated distillation of the resulting hydrocarbon product is shown in Figure 11. A major fraction of the hydrocarbon products equal to ~75% lie in the 150 to 300°C boiling point span, which is within the jet-fuel range. This integrated catalytic approach appears as a likely renewable energy process for producing aviation fuels. Note that the compatibility of the hydrocarbon products with jet fuel could be further improved by tuning the process conditions for the oligomerization step and obtaining a higher  $\text{C}_{16}$ : $\text{C}_8$  olefins ratio. This could also be accomplished by recycle of the light olefins (e.g.,  $\text{C}_7$  and  $\text{C}_8$ ) in the oligomerization step which would assist in increasing chain growth.<sup>42</sup>

### **Carbon efficiency for the integrated process**

A summary of the process conditions and carbon efficiencies for each step within the integrated syngas-to-jet range hydrocarbon process presented in Figure 1 (case B) is shown in

Table 8. Complete techno-economic analysis for the integrated process is being performed which will assess overall energy efficiency as well as provide a cost analysis. Here we consider the carbon efficiency for each of the catalytic steps presented in the integrated process. In the Rh-catalyzed syngas conversion step approximately 73% of the converted carbon forms the condensable mixed oxygenates shown in Table 2 (primary constituents include ethanol, acetic acid, acetaldehyde, and ethyl acetate).<sup>16</sup> The rest of the converted carbon include primarily light hydrocarbons<sup>16</sup> that would be utilized as fuel gas. It should be noted that unreacted syngas would be recycled to the mixed oxygen synthesis reactor. Resulting aqueous mixed oxygenate mixture was demonstrated to produce C<sub>3</sub>-C<sub>5</sub> olefins over Zn<sub>1</sub>Zr<sub>10</sub>O<sub>z</sub> with approximately 59% yield for the conditions as reported in Figure 4 (450°C, 15 bar, 340 h<sup>-1</sup>). The vast majority of the additional carbon is lost as CO<sub>2</sub> (~33% yield) as a consequence of the ketonization reaction (see Figure 2). The C<sub>3</sub>-C<sub>5</sub> olefins were quite selectively oligomerized to a C<sub>7</sub>-C<sub>16</sub> olefin using Amberlyst-36 solid acid resin (95% yield) under the conditions as shown in Table 6 (140°C, 21 bars, 0.446 h<sup>-1</sup>). Hydrotreatment is then necessary to produce a saturated hydrocarbon suitable for jet blendstock. Simulated distillation indicate approximately 75% of the oligomerized product to be in the jet range, however, optimization of the oligomerization could improve yield to jet, for example, recycle of the lighter C<sub>7</sub> and C<sub>8</sub> olefins would further increase chain growth.

For the integrated process we demonstrate an overall carbon selectivity of approximately 41%. As discussed above significant carbon loss occurs as a result of the ketonization reaction that occurs within the oxygenate-to-olefin conversion step. For this reason we are currently exploring alternative C-C coupling reactions such as Guerbet coupling of ethanol<sup>43, 44</sup> that after dehydration also produce a C<sub>4</sub> olefin but without the stoichiometric requirement of CO<sub>2</sub>

production. An overarching benefit of  $C_4$  olefin oligomerization is that resulting carbon length can be readily tailored to desired transportation fuel specification.

## Conclusion

Efficient conversion of biomass derived syngas into drop-in fuels was demonstrated with a novel integrated catalytic process consisting of four chemical reactors operating in series. The approach first converts syngas into a complex mixture of  $C_2^+$  oxygenates that then are transformed into an isobutene-rich olefin mixture. Oligomerization of the light olefin mixture leads to a high yield (>80%) of  $C_7^+$  olefins that are then hydrogenated, ultimately resulting in a high molecular weight paraffin product. Oligomerization of light olefins enables process flexibility in the production of diesel- and/or jet-fuel range hydrocarbons. Overall, we demonstrate a carbon efficiency of approximately 41% for this integrated syngas-to-jet range hydrocarbon process. While applicable to syngas, the upgrading technology offered by the  $Zn_xZr_yO_z$  mixed-oxide type catalyst also offers tremendous versatility as it can accommodate a variety of  $C_2^+$  oxygenated feedstocks. For example, cheaper feedstocks such as ethanol and acetic acid that are derived from the fermentation of carbohydrates could be used in lieu of syngas.

## Acknowledgements

This work was financially supported by the U.S. Department of Energy (DOE) Bioenergy Technologies Office (BETO) and performed at Pacific Northwest National Laboratory (PNNL). PNNL is a multi-program national laboratory operated for DOE by Battelle Memorial Institute. Advanced catalyst characterization use was granted by a user proposal at the William R. Wiley Environmental Molecular Sciences Laboratory (EMSL). EMSL is a national scientific user

facility sponsored by DOE's Office of Biological and Environmental Research and located at PNNL. The authors would like to thank Teresa Lemmon and Marie Swita for analytical support of this project. Finally, the authors would also like to thank Cary Counts for help with technical editing of this manuscript.

**Table 1.** Summary of Test Condition used for Stability Evaluation of PNNL Rh-Based Catalyst Previously Developed for the Conversion of Syngas to Mixed Oxygenates. Reprinted with Permission from Reference 16.<sup>16</sup>

Catalyst ID	H-A
Pressure	83 bar
Temperature	260°C
Gas Composition <sup>a</sup>	1.3/1.0 H <sub>2</sub> /CO Ratio with 3.4% N <sub>2</sub> , 3.4% CO <sub>2</sub>
GHSV	13,000 L/kg <sub>cat</sub> /hr
Time Online before Long-Term Test	267 hours
Total Time at Test Conditions	2,373 hours

<sup>a</sup> The nominal feed gas was achieved by mixing a measured flowrate of a gas mixture containing 2/1 H<sub>2</sub>/CO ratio with 4% N<sub>2</sub>, 4% CO<sub>2</sub>, with a separate flowrate of 100% CO to achieve the desired 1.3/1 H<sub>2</sub>/CO ratio. There were periods when the mixture was achieved by mixing separate flowrates of pure CO, pure H<sub>2</sub> and pure N<sub>2</sub> at rates to achieve a 1.3:1 H<sub>2</sub>:CO ratio with 8% N<sub>2</sub>.

**Table 2.** Composition of the Mixed Oxygenate Product Obtained from Syngas Conversion over the Rh-Based Catalyst. Smaller amounts of minor oxygenate products are not reported here (<2 wt% total).

Component	wt%
Methanol	0.8
Ethanol	20.5
1-Propanol	0.8
1-Butanol	0.8
1-Pentanol	0.2
Acetic Acid	10.0
Acetaldehyde	10.5
Ethyl Acetate	9.9
Water	46.5
Sum	100.0



**Table 3.** Oligomerization of Isobutene over HY, HZSM-5, and Amberlyst-36 Catalysts. Feed composition: 70% isobutene, 30% N<sub>2</sub>.

Catalyst	HY	HZSM-5	Amberlyst-36
Reaction temperature ( °C)	250	250	140
WHSV (h <sup>-1</sup> )	1.3	1.1	1.3
Time-on-stream (hours)	21	17	31
Conversion (%)	100	100	100
Selectivities (%)			
C <sub>1</sub> –C <sub>6</sub> olefins	13.4	4.7	0
C <sub>1</sub> –C <sub>6</sub> paraffins	6.4	20.9	0
C <sub>7</sub> –C <sub>12</sub> olefins	67.9	26.9	49.9
C <sub>7</sub> –C <sub>12</sub> paraffins	6.2	47.5	1.5
C <sub>16</sub> <sup>+</sup> olefins	0	0	14.6
C <sub>8</sub> –C <sub>12</sub> cyclic hydrocarbons	6.1	0	34.0
C <sub>7</sub> <sup>+</sup> yield	80.2	74.4	98.4

**Table 4.** Hydrocarbons Product Distribution for Oligomerization of Olefins with Reaction Conditions Reported in Figure 9. Catalyst: Amberlyst-36, T = 140°C. The carbon balance for the whole process is between 76-83% depending on the reaction conditions.

WHSV (h <sup>-1</sup> )	Pressure (bar)	Hydrocarbon products distribution (%)		
		C <sub>1</sub> –C <sub>6</sub> olefins + paraffins	C <sub>7</sub> –C <sub>12</sub> olefins + paraffins <sup>a</sup>	C <sub>8</sub> –C <sub>12</sub> cyclic hydrocarbons
0.1	7	46.2	46.6	7.3
0.05	7	41.1	51.8	7.1
0.1	14	23.9	67.7	8.4

<sup>a</sup> Less than 3% paraffin**Table 5.** Composition of the Olefin Mixture used as a Feed for Oligomerization Reactor R3.

Olefins Mixture	Propene (mol%)	Isobutene (mol%)	Pentene (mol%)
Mixture A	10.8	77.3	11.9
Mixture B	19.2	75.8	4.1

**Table 6.** Selectivities for the Oligomerization of Olefin Mixture over Amberlyst-36 at T = 140°C, P = 21 bars and Conversion = 100%. The carbon balance for the whole process is between 90-98% depending on the reaction conditions.

Olefin Mixture	WHSV (h <sup>-1</sup> )	Selectivities (%)			
		C <sub>1</sub> -C <sub>6</sub> olefins	C <sub>7</sub> -C <sub>12</sub> olefins + paraffins <sup>a</sup>	C <sub>12</sub> <sup>+</sup> olefins <sup>b</sup>	C <sub>8</sub> -C <sub>12</sub> cyclic hydrocarbons
Mixture A	0.378	12.7 <sup>c</sup>	52.3	15.3	19.7
Mixture B	0.223	11.1	49.2	13.9	25.8
	0.446	4.9	58.4	5.9	30.8
	0.891	2.8	64.9	4.0	28.3

<sup>a</sup> Less than 2% paraffins,  
<sup>b</sup> mostly C<sub>13</sub>-C<sub>16</sub> olefins  
<sup>c</sup> half olefins and half paraffins

**Table 7.** Influence of the carrier gas on the conversion and selectivities for the oligomerization of isobutene over Amberlyst-36 at T = 140°C, WHSV = 20 h<sup>-1</sup> and P = 7 bar. Isobutene = 70% and balance carrier gas (N<sub>2</sub> or H<sub>2</sub> or CO<sub>2</sub>) = 30%.

Feed	Conversion (%)	Selectivities (%)			
		C <sub>1</sub> -C <sub>6</sub> olefins	C <sub>7</sub> -C <sub>12</sub> olefins	C <sub>16</sub> olefins	C <sub>8</sub> -C <sub>12</sub> cyclic hydrocarbons
isobutene + N <sub>2</sub>	89	3.0	77.7	9.8	9.5
isobutene + H <sub>2</sub>	87	3.2	75.6	10.6	10.6
Isobutene +	87	4.4	79.2	6.9	9.5

CO<sub>2</sub>**Table 8.** Process condition summaries and carbon efficiencies for each step within the integrated syngas-to-jet range hydrocarbon process depicted in Figure 1 “case B”.

Catalytic Step <sup>a</sup>	Conversion (%)	Catalyst	Conditions	Reference	Carbon Efficiency (%)
Mixed Oxygenate Synthesis (from syngas)	~ 30 (single pass)	Rh-based	T = 260°C P = 83 bar GHSV ~ 13,000 h <sup>-1</sup>	Ref 16	73 <sup>b</sup>
Olefin Production	100	Zn <sub>1</sub> Zr <sub>10</sub> O <sub>z</sub>	T = 450°C P = 15 bar GHSV = 340 h <sup>-1</sup>	This work, Figure 5	59 <sup>c</sup>
Oligomerization	100	Amberlyst-36	T = 140°C P = 21 bar WHSV = 0.446 h <sup>-1</sup>	This work, Table 6	95 <sup>d</sup>
Hydrotreatment	100	3%Pt/Al <sub>2</sub> O <sub>3</sub>	T = 260°C P = 52 bar	This work	~100 <sup>e</sup>
TOTAL					41 <sup>f</sup>

<sup>a</sup> Demonstrated using bench-scale continuous flow reactors except for the more conventional hydrotreatment step which was performed in a batch reactor.

<sup>b</sup> Carbon selectivity to the condensable mixed oxygenate products shown in Table 2.

<sup>c</sup> Carbon selectivity to propene (17.9%), butenes (34.3%), and pentenes (7.1%).

<sup>d</sup> Selectivity to C<sub>7</sub><sup>+</sup> olefins. Note that in application recycle of the C<sub>7</sub> and C<sub>8</sub> olefins would likely be necessary in the oligomerization step in order to further increase chain growth.

<sup>e</sup> Olefin saturation selectivity.

<sup>f</sup> Approximate overall carbon selectivity for the conversion of syngas to C<sub>7</sub>-C<sub>16</sub> saturated hydrocarbons.

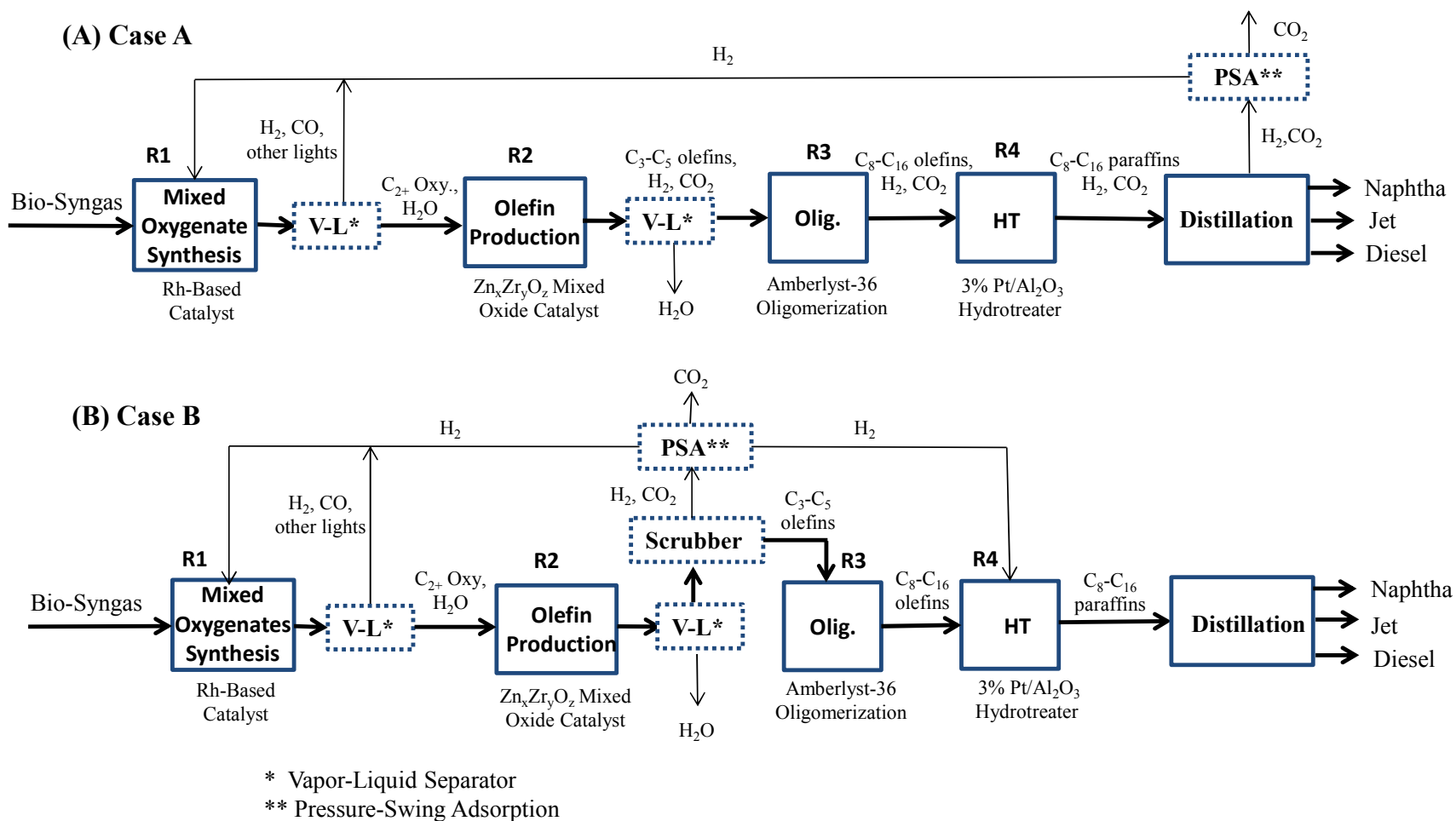


**Figure 1.** Schematic Representations for Two Cases, Each with Different Separation Schemes, for the Integrated Processes of Catalytic Conversion of Biomass-Derived Syngas into Transportation Fuels (with major intermediates identified).



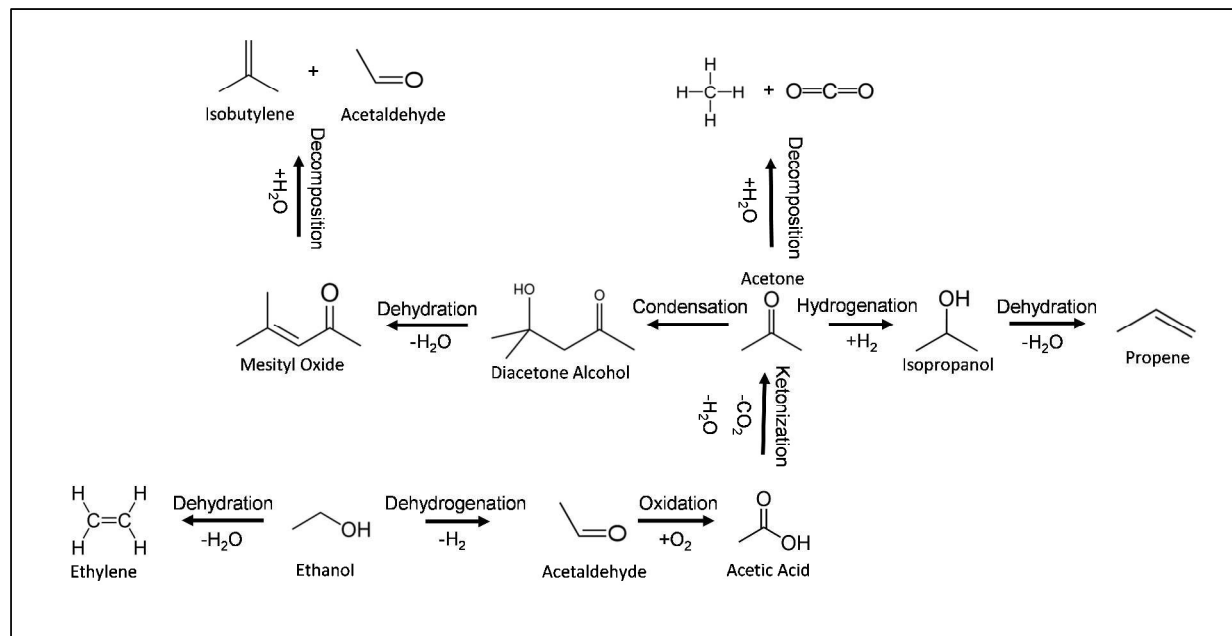


**Figure 2.** Simplified reaction network for the conversion of ethanol to isobutene (and major side products). Reprinted with permission from Reference 22.

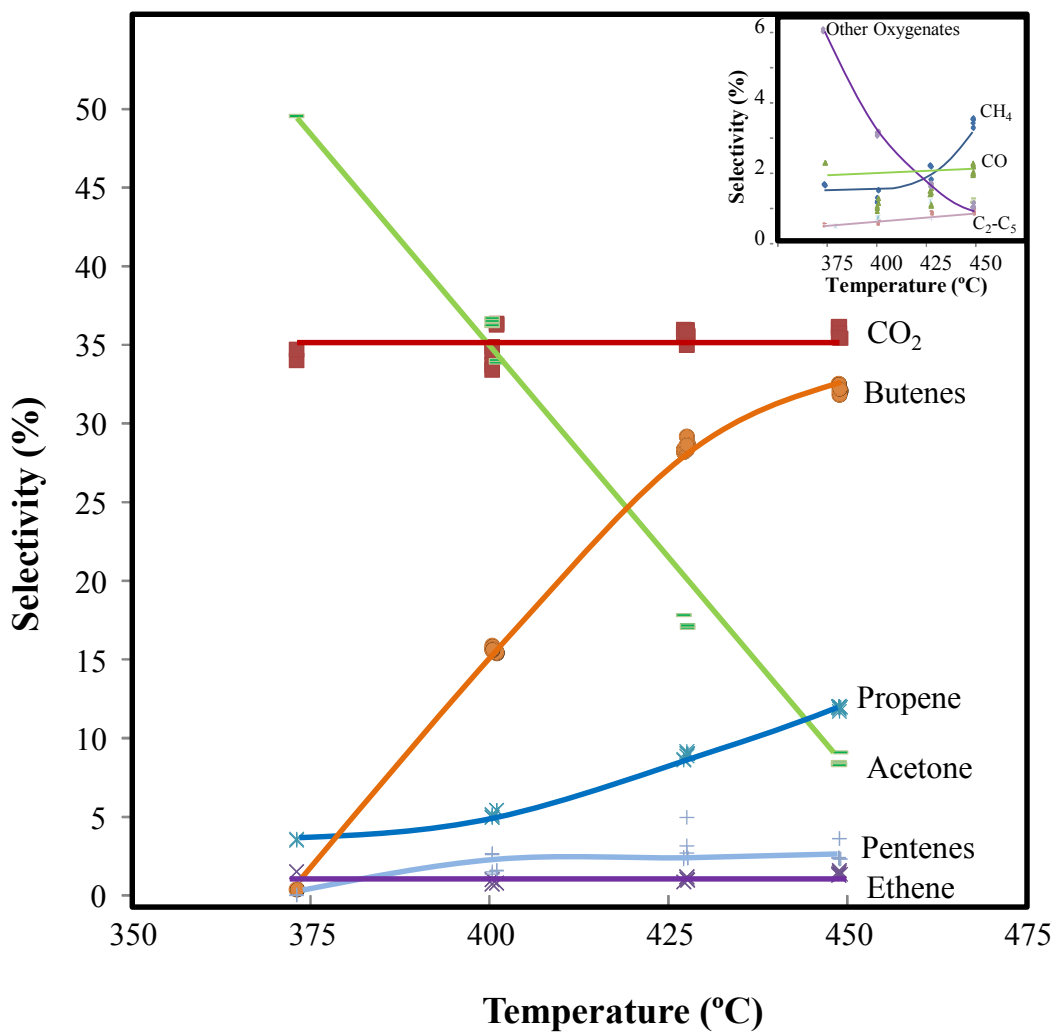


**Figure 3.** Effect of Temperature on the Selectivity for Conversion of Mixed Oxygenates (40% in N<sub>2</sub>) to Olefins in Reactor R2 and over Zn<sub>1</sub>Zr<sub>10</sub>O<sub>z</sub>. Selectivity to minor products is presented in the insert. Conversion  $\geq 94\%$ , GHSV = 3,700 h<sup>-1</sup>, P = 21 bar. The other oxygenates consists primarily of 2-butanone and C<sub>2</sub>-C<sub>5</sub> are alkanes.

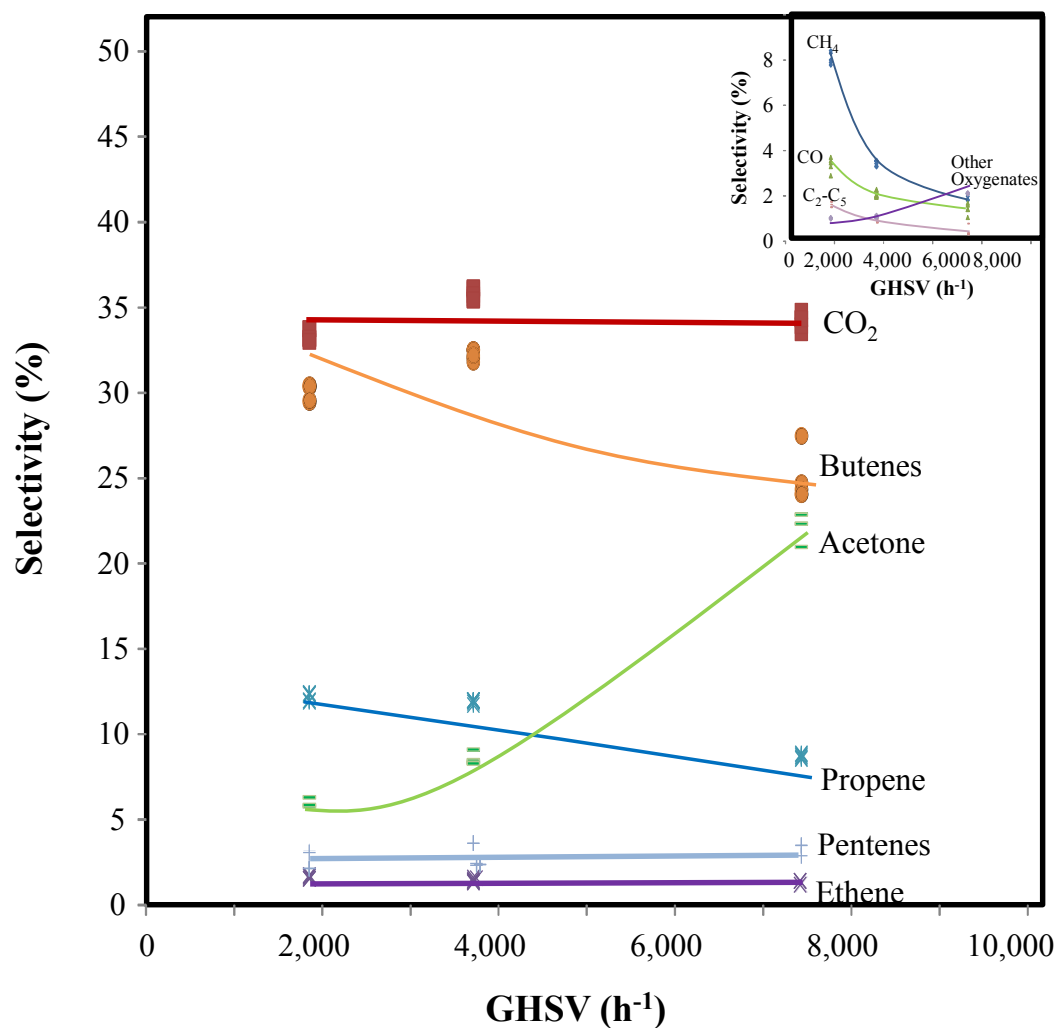


**Figure 4.** Effect of GHSV on Selectivity for Conversion of Mixed Oxygenates (40% in N<sub>2</sub>) to Olefins in Reactor R2 and over Zn<sub>1</sub>Zr<sub>10</sub>O<sub>2</sub>. Selectivity to minor products is presented in the insert. Conversion = 100%, T = 450°C, P = 21 bar. The other oxygenates consists of 2-butanone and C<sub>2</sub>-C<sub>5</sub> are alkanes.



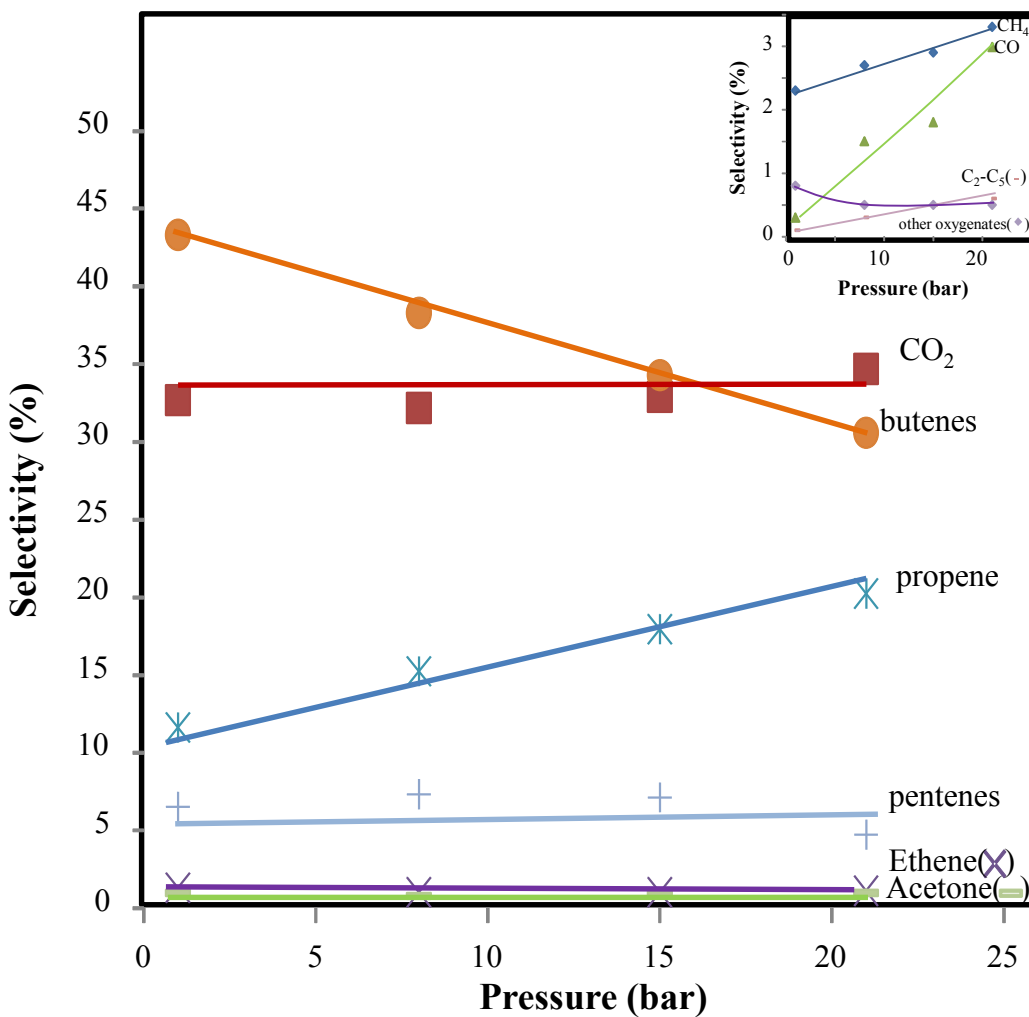


**Figure 5.** Effect of Pressure on Selectivity for Conversion of Mixed Oxygenates (60% in N<sub>2</sub>) to Olefins in Reactor R2 and over Zn<sub>1</sub>Zr<sub>10</sub>O<sub>z</sub>. Selectivity to minor products is presented in the insert. Conversion = 100%, T = 450°C, GHSV = 340 h<sup>-1</sup>. The other oxygenates consists of 2-butanone and C<sub>2</sub>-C<sub>5</sub> are alkanes.

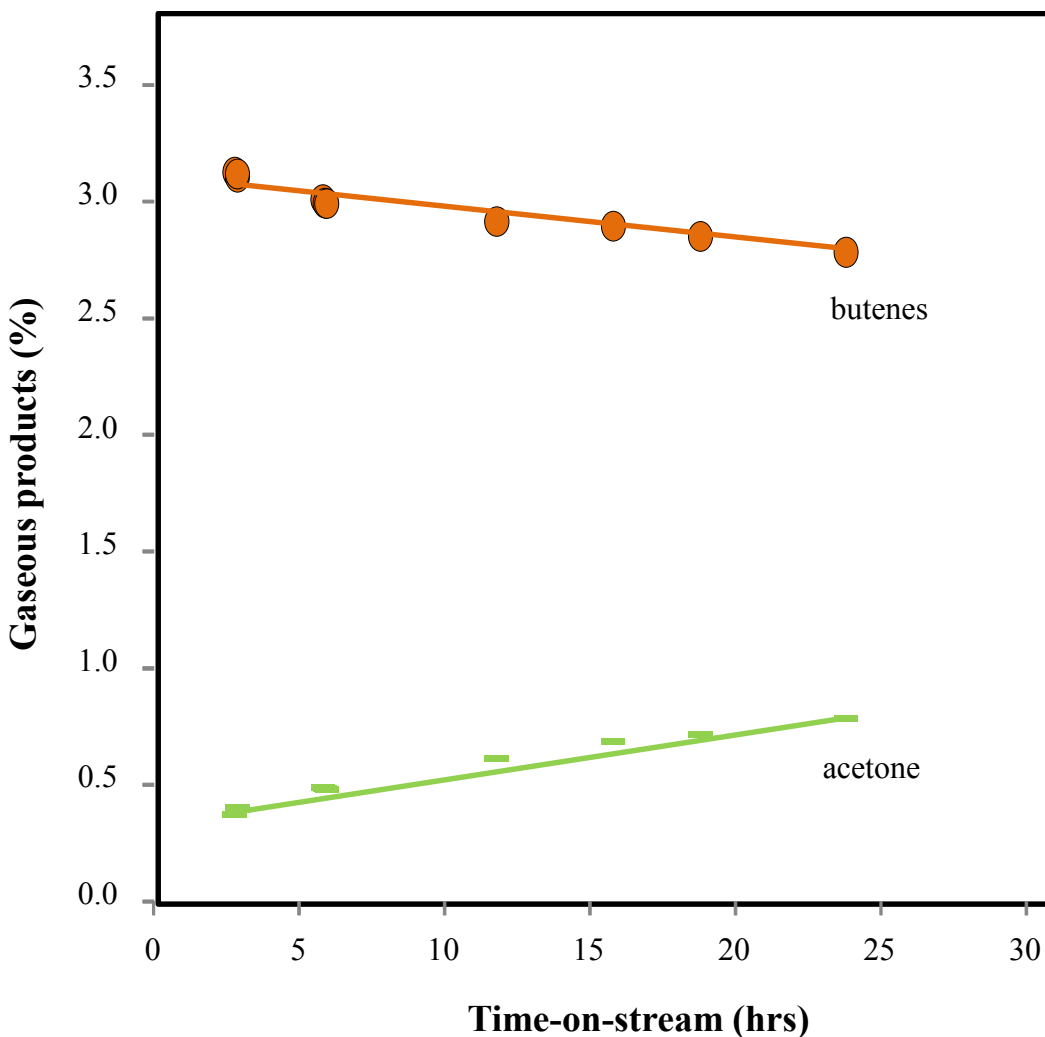


**Figure 6.** Evolution of Butenes (consisting of predominantly isobutene) and Acetone Production with TOS for the Conversion of Mixed Oxygenates (40% in  $N_2$ ) to Olefins in Reactor R2 and over  $Zn_1Zr_{10}O_z$ .  $T = 450^\circ C$ ,  $P = 1 \text{ bar}$ ,  $GHSV = 3700 \text{ h}^{-1}$ .

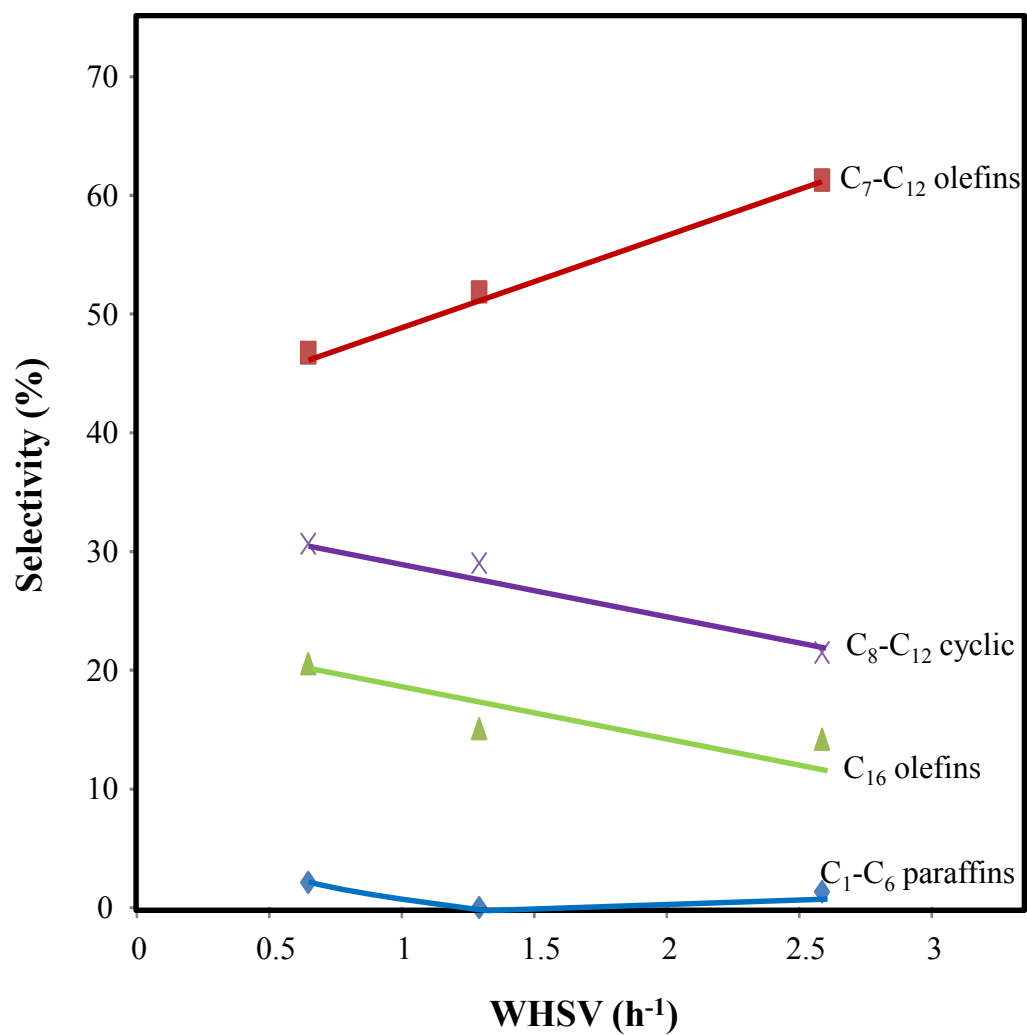


**Figure 7.** Evolution of the Selectivity for Isobutene Oligomerization over the Amberlyst-36 Catalyst as a Function of WHSV, T = 140°C, P = 17 bar, Conversion = 100%, Isobutene/N<sub>2</sub> (molar) = 70/30.

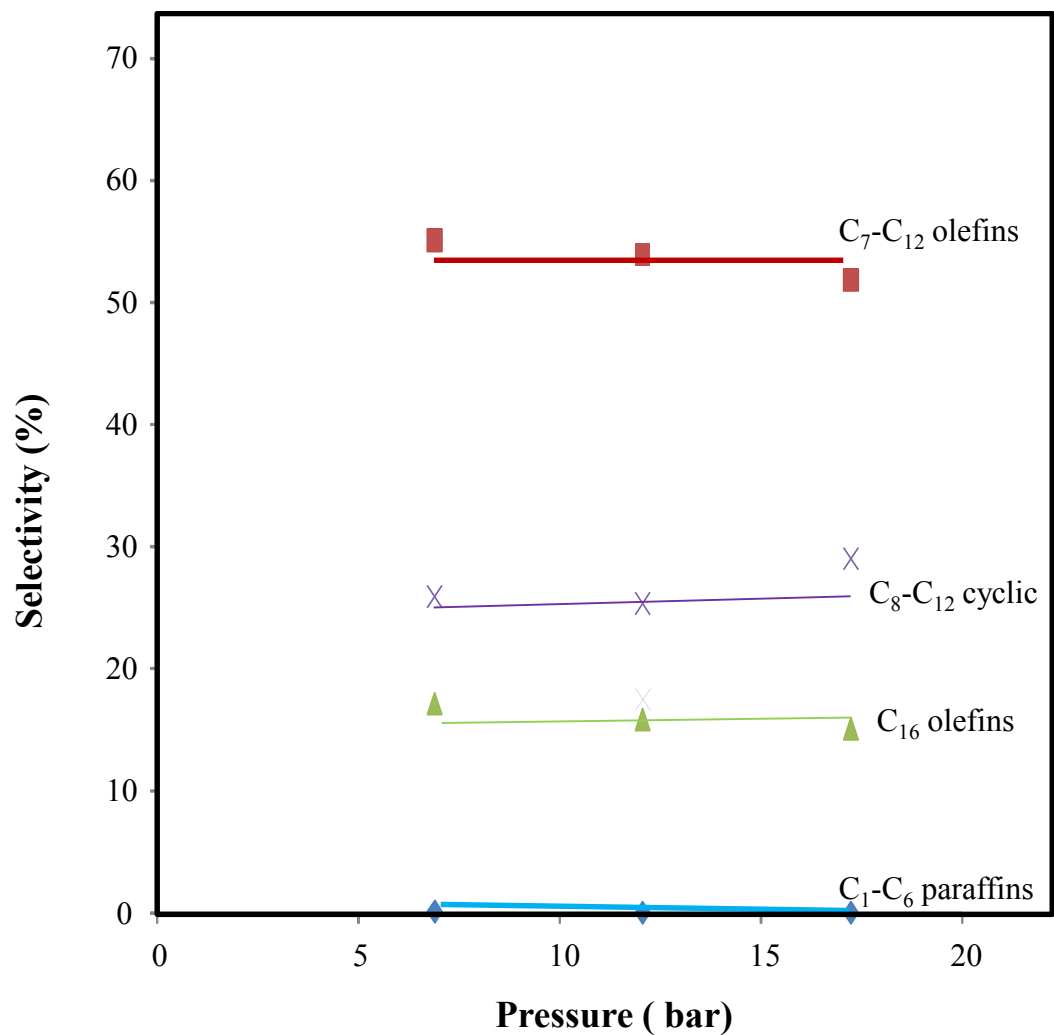


**Figure 8.** Evolution of the Selectivity for Isobutene Oligomerization over the Amberlyst-36 Catalyst as a Function of the Pressure.  $T = 140^{\circ}\text{C}$ ,  $\text{WHSV} = 1.3 \text{ h}^{-1}$ , conversion = 100%, isobutene/ $\text{N}_2$  (molar) = 70/30.

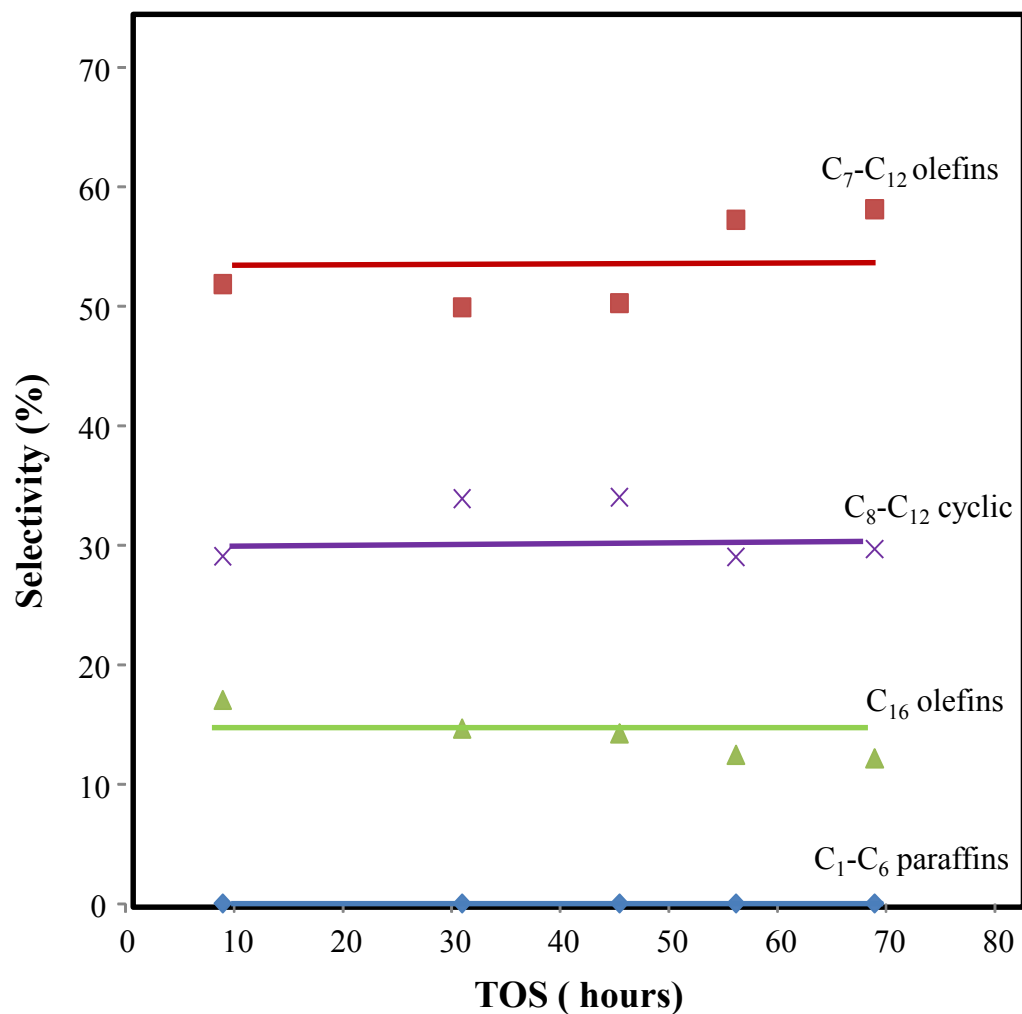


**Figure 9.** Evolution of the Selectivity with TOS for Isobutene Oligomerization over Amberlyst-36. T = 140°C, P = 17 bar, WHSV = 1.3 h<sup>-1</sup>, conversion = 100%, isobutene/N<sub>2</sub> (molar) = 70/30.

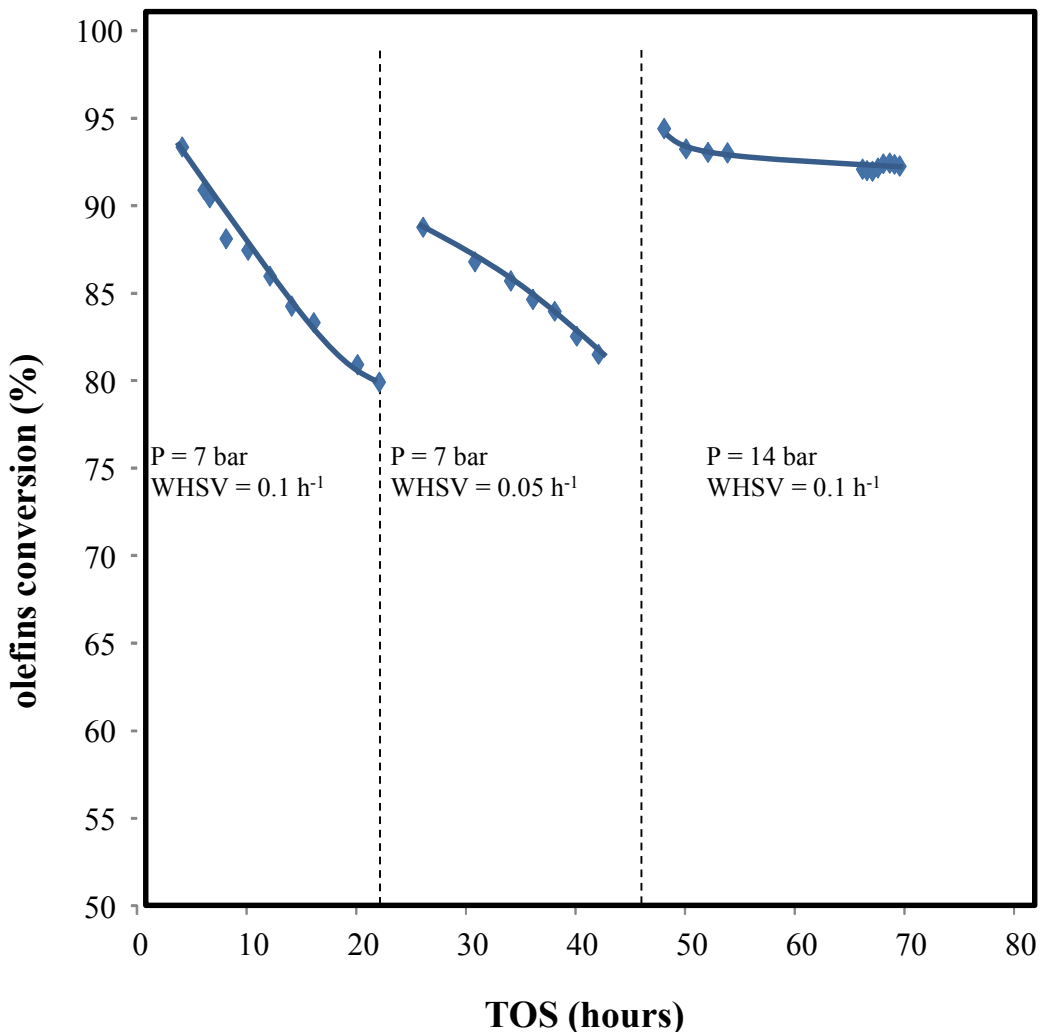


**Figure 10.** Evolution of the Olefins Conversion with TOS for the Oligomerization of Olefins from Reactor R2 (“case A”). Catalyst: Amberlyst-36. Feed composition: H<sub>2</sub>=33%, CO<sub>2</sub>=13%, butenes =3- 4.2%, propene = 2%, pentenes = 1-3.5%, CO =0.6-0.9%, traces of ethane and propane (<0.03%), balance N<sub>2</sub>. T = 140°C, P = 7-14 bar, WHSV = 0.05-0.1 h<sup>-1</sup>.

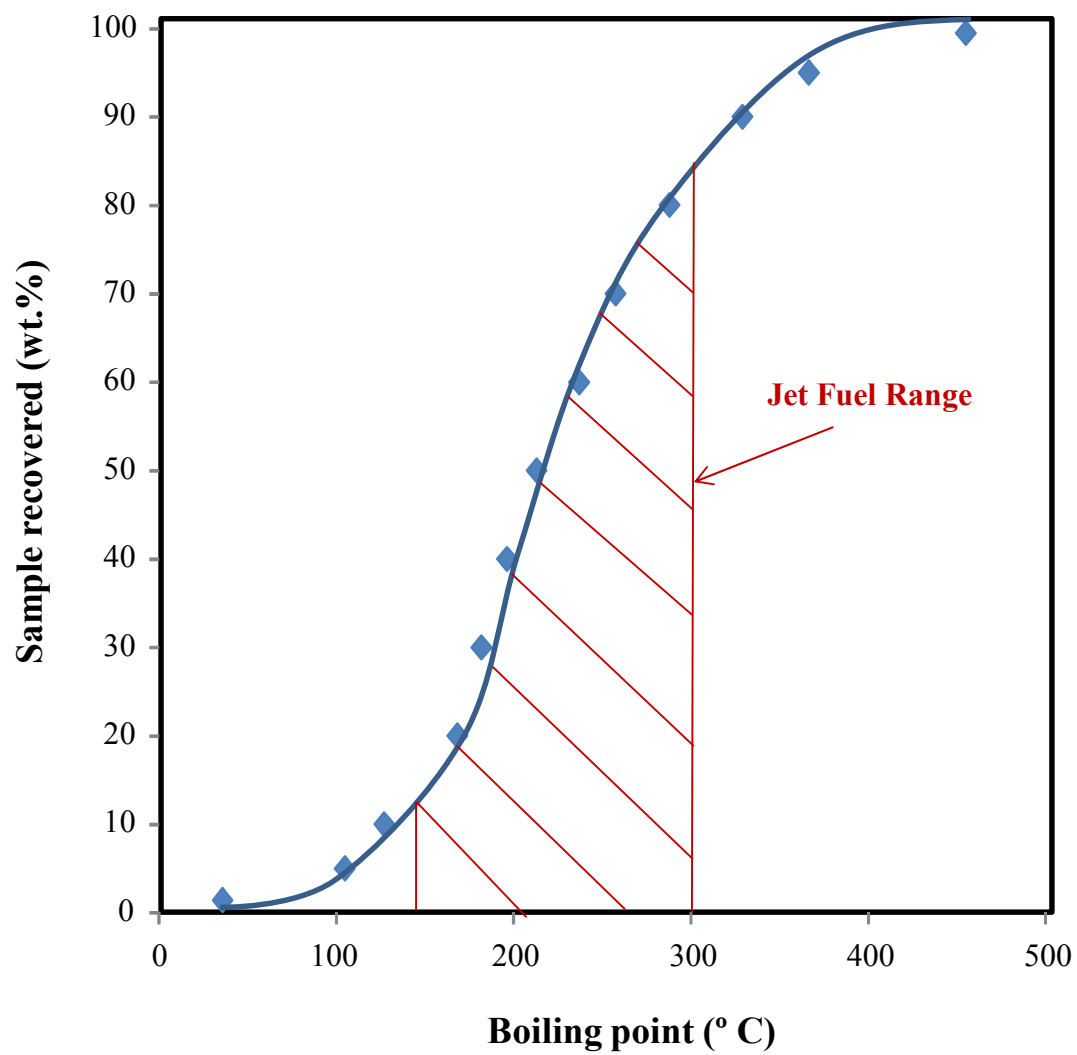


**Figure 11.** Simulated Distillation Profile of the Hydrotreated Fraction (post-Reactor R4).

## References

1. G. W. Huber, S. Iborra and A. Corma, *Chemical Reviews*, 2006, **106**, 4044-4098.
2. D. M. Alonso, J. Q. Bond and J. A. Dumesic, *Green Chemistry*, 2010, **12**, 1493-1513.
3. R. C. Brown, *Thermochemical Processing of Biomass: Conversion into Fuels, Chemicals and Power*, 2011.
4. S. Czernik and A. V. Bridgwater, *Energy Fuels*, 2004, **18**, 590-598.
5. J. Holladay, Thermochemical Conversion Processes to Aviation Fuels-Advanced Bio-based Jet Fuel Cost of Production Workshop, [http://energy.gov/sites/prod/files/2014/04/f14/holladay\\_caafi\\_workshop.pdf](http://energy.gov/sites/prod/files/2014/04/f14/holladay_caafi_workshop.pdf).
6. A. Coelho, G. Caeiro, M. A. N. D. A. Lemos, F. Lemos and F. R. Ribeiro, *Fuel*, 2013, **111**, 449-460.
7. Peters, M. W.; Taylor, J. Renewable Jet Fuel Blendstock from Isobutanol. USA Patent, US 8373012.
8. Honeywell, <http://honeywell.com/News/Pages/Honeywell%E2%80%99s-UOP-Receives-Contract-To-Demonstrate-Technology-For-Conversion-Of-Alcohol-To-Aviation-Biofuel.aspx>.
9. Cobalt, <http://www.cobalttech.com/biojetfuel.html>.
10. J. Q. Bond, D. M. Alonso, D. Wang, R. M. West and J. A. Dumesic, *Science*, 2010, **327**, 1110-1114.
11. J. Hu, Y. Wang, C. Cao, D. C. Elliott, D. J. Stevens and J. F. White, *Catalysis Today*, 2007, **120**, 90-95.
12. J. Yu, D. Mao, L. Han, Q. Guo and G. Lu, *Journal of Molecular Catalysis A: Chemical*, 2013, **367**, 38-45.
13. J. G. Nunan, C. E. Bogdan, K. Klier, K. J. Smith, C.-W. Young and R. G. Herman, *Journal of Catalysis*, 1989, **116**, 195-221.
14. J. Liu, R. Tao, Z. Guo, J. R. Regalbuto, C. L. Marshall, R. F. Klie, J. T. Miller and R. J. Meyer, *ChemCatChem*, 2013, **5**, 3665-3672.
15. J. J. Spivey and A. Egbebi, *Chemical Society Reviews*, 2007, **36**, 1514-1528.
16. M.A Gerber, M.J. Gray, B.L. Thompson, *Long-Term Testing of Rhodium-Based Catalysts for Mixed Alcohol Synthesis*, Pacific Northwest National Laboratory Report, 2013, PNNL-22786..
17. D. Mei, R. Rousseau, S. M. Kathmann, V.-A. Glezakou, M. H. Engelhard, W. Jiang, C. Wang, M. A. Gerber, J. F. White and D. J. Stevens, *Journal of Catalysis*, 2010, **271**, 325-342.
18. V. A. Glezakou, J. E. Jaffe, R. Rousseau, D. H. Mei, S. M. Kathmann, K. O. Albrecht, M. J. Gray and M. A. Gerber, *Topics in Catalysis*, 2012, **55**, 595-600.
19. K. K. Ramasamy, M. A. Gerber, M. Flake, H. Zhang and Y. Wang, *Green Chemistry*, 2014, **16**, 748-760.
20. J. Sun, K. Zhu, F. Gao, C. Wang, J. Liu, C. H. F. Peden and Y. Wang, *Journal of the American Chemical Society*, 2011, **133**, 11096-11099.
21. C. Liu, J. Sun, C. Smith and Y. Wang, *Applied Catalysis A: General*, 2013, **467**, 91-97.
22. C. Smith, V. Dagle, M. Flake, K. Ramasamy, L. Kovarik, M. Bowden, T. Onfroy and R. Dagle, *Catalysis Science & Technology*, 2016, DOI: 10.1039/C5CY01261A
23. V. M. Lebarbier, A. M. Karim, M. H. Engelhard, Y. Wu, B.-Q. Xu, E. J. Petersen, A. K. Datye and Y. Wang, *ChemSusChem*, 2011, **4**, 1679-1684.



24. Sun, J.; Liu, C.; Wang, Y.; Smith, C. Stable mixed oxide catalysts for direct conversion of ethanol to isobutene and process for making. USA Patent, US 20150217273
25. M.A. Gerber, M.J. Gray, K.O. Albrecht, B.L. Thompson, *Optimization of Rhodium-Based Catalysts for Mixed Alcohol Synthesis – 2012 Progress Report*, Pacific Northwest National Laboratory Report, 2012, PNNL-22659.
26. J. Sun, R. A. L. Baylon, C. Liu, D. Mei, K. J. Martin, P. Venkitasubramanian and Y. Wang, *Journal of the American Chemical Society*, 2015, DOI: 10.1021/jacs.5b07401.
27. R. S. Murthy, P. Patnaik, P. Sidheswaran and M. Jayamani, *Journal of Catalysis*, 1988, **109**, 298.
28. T. Nakajima, H. Nameta, S. Mishima, I. Matsuzaki and K. Tanabe, *Journal of Materials Chemistry*, 1994, **4**, 853.
29. A. I. Biaglow, J. Sepa, R. J. Gorte and D. White, *Journal of Catalysis*, 1995, **151**, 373-384.
30. A. G. Panov and J. J. Fripiat, *Journal of Catalysis*, 1998, **178**, 188-197.
31. T. Tago, H. Konno, S. Ikeda, S. Yamazaki, W. Ninomiya, Y. Nakasaka and T. Masuda, *Catalysis Today*, 2011, **164**, 158-162.
32. K. Hauge, E. Bergene, D. Chen, G. R. Fredriksen and A. Holmen, *Catalysis Today*, 2005, **100**, 463-466.
33. J. Q. Bond, A. A. Upadhye, H. Olcay, G. A. Tompsett, J. Jae, R. Xing, D. M. Alonso, D. Wang, T. Y. Zhang, R. Kumar, A. Foster, S. M. Sen, C. T. Maravelias, R. Malina, S. R. H. Barrett, R. Lobo, C. E. Wyman, J. A. Dumesic and G. W. Huber, *Energy & Environmental Science*, 2014, **7**, 1500-1523.
34. B. Nkosi, F. T. T. Ng and G. L. Rempel, *Applied Catalysis A: General*, 1997, **158**, 225-241.
35. J. F. Izquierdo, M. Vila, J. Tejero, F. Cunill and M. Iborra, *Applied Catalysis A: General*, 1993, **106**, 155-165.
36. G. Bellussi, F. Mizia, V. Calemma, P. Pollesel and R. Millini, *Microporous and Mesoporous Materials*, 2012, **164**, 127-134.
37. C. Gutiérrez-Antonio, F. I. Gómez-Castro, S. Hernández and A. Briones-Ramírez, *Chemical Engineering and Processing: Process Intensification*, 2015, **88**, 29-36.
38. J. A. Widegren and T. J. Bruno, *Industrial & Engineering Chemistry Research*, 2008, **47**, 4342-4348.
39. E. Gianotti, Á. Reyes-Carmona, K. Pearson, M. Taillades-Jacquín, G. Kraaij, A. Wörner, J. Rozière and D. J. Jones, *Applied Catalysis B: Environmental*, 2015, **176–177**, 480-485.
40. *ASTM D7566*.
41. X. Zhang, J. Zhong, J. Wang, L. Zhang, J. Gao and A. Liu, *Fuel Processing Technology*, 2009, **90**, 863-870.
42. W.-C. Wang and L. Tao, *Renewable and Sustainable Energy Reviews*, 2016, **53**, 801-822.
43. J. T. Kozlowski and R. J. Davis, *ACS Catalysis*, 2013, **3**, 1588-1600.
44. K. Ramasamy, M. Gray, H. Job, D. Santosa, X. Li, A. Devaraj, A. Karkamkar and Y. Wang, *Topics in Catalysis*, 2015, DOI: 10.1007/s11244-015-0504-8, 1-9.